Pergamon

Materials Research Bulletin 35 (2000) 1023–1033

Materials Research Bulletin

Study of the phases in a copper cathode during an electrodeposition process for obtaining Cu–Li alloys

O.A. Lambri[a,*], J.I. Pérez-Landazábal[b], A. Peñaloza[c], O. Herrero[d], V. Recarte[b], M. Ortiz[c], C.H. Wörner[c]

[a]*Laboratorio de Materiales, Escuela de Ingeniería Eléctrica, Facultad de Ciencias Exactas, Ingeniería y Agrimensura, Universidad Nacional de Rosario, National Council of Research (CONICET), Instituto de Física Rosario, Avda. 27 de febrero 210 bis, (2000) Rosario, Argentina*
[b]*Dpto. de Física, Universidad Pública de Navarra, Campus de Arrosadia s/n, 31006 Pamplona, Spain*
[c]*Instituto de Física, Universidad Católica de Valparaíso, Avda. Brasil 2950, Valparaíso, Chile*
[d]*Dirección de Asesoramiento Técnico de la Provincia de Santa Fe (DAT), Esmeralda y Ocampo, (2000) Rosario, Argentina*

(Refereed)
Received 26 July 1999; accepted 21 September 1999

Abstract

The evolution of Cu–18at%Li crystals, Cu_2O, Li_2CO_3, and CuO phases, which nucleate and grow during the electrodeposition process in a copper cathode, was examined. The electrodeposition process was mainly responsible for promoting the formation of copper oxides and lithium-carbonates in the cathode. The evolution of both the quantity of Cu–Li crystals formed at the surface of the cathode and the total lithium concentration of the sample as a function of the electrodeposition time was studied.

Keywords: A. Alloys; C. X-ray diffraction; D. Phase equilibria

1. Introduction

Several copper alloys are widely employed as electrical materials in different applications, e.g., conductors and switches. One of them is the Cu–Be alloy. It has been widely studied due

* Corresponding author. Fax: + 54-341-482-17-72.
E-mail address: olambri@fceia.unr.edu.ar (O.A. Lambri).

0025-5408/00/$ – see front matter
PII: S0025-5408(00)00313-5

to its excellent mechanical properties, high electrical conductivity, and high corrosion resistance [1–7]. In addition, the mechanical behavior of Cu–Be alloys can be improved by the addition of Zr [8]. Another recently studied copper alloy, which has a light atom and exhibits good mechanical behavior, is the copper–lithium alloy produced by electrodeposition. Results from previous work on the behavior of damping and elastic modulus [9] and precipitation processes related to age-hardening [10] have been reported. In that work, the main effort was directed towards examining the microstructural evolution of Cu–Li alloy in relation to its mechanical behavior. A careful study of the phases that appear during the electrodeposition process has not been reported. In the present work, the effects of the electrodeposition process on the copper cathode were studied by X-ray diffraction technique. The appearance of new phases of Cu–18at%Li Cu_2O, Li_2CO_3, and CuO and their increase in concentration as a function of the electrodeposition time was determined. The control of these phases is worthy of further study from the point of view of technological development of parts from compacted Cu–18at%Li powders. The quantity of such powders during electrodeposition was also studied.

2. Experimental

Copper–lithium alloys were obtained by electrodeposition technique, using a sheet ($50 \times 25 \times 0.1$ mm^3) of high-purity copper (99.99%) as the cathode and a similar size sheet of graphite as the anode [11]. Electrodeposition was carried out in a bath of fused salts of lithium (LiCl) and potassium (KCl), at constant temperature of about 753 K. Both electrodes were vertically positioned inside the fused salts, parallel to each other, with a gap of 10 mm between them. A constant current of 1.5 A was employed. When the electrodeposition process was completed, after different periods of time, the samples were washed in water at room temperature to remove the excess of lithium. They were subsequently stored in air at room temperature for greater than 300 h. The cathode exhibited a yellow surface with powders of a dendritic distribution as shown in Fig. 1. The Cu–Li powders that formed on the surface of the cathode had a composition of about 18 at% Li, a fcc structure, and a slightly larger lattice parameter (0.364 nm) than that of pure copper (0.361 nm) [9,10]. Fig. 2 shows the geometrical characteristics of the Cu–Li crystals formed on the cathode. This seems to indicate that the dendrites were composed of small single-crystals of cubic shape, as evident from their crystal faces. An atomic absorption analysis was carried out to determine whether impurities such as potassium and sodium were present in the Cu–18at%Li powders. Since Li, Na, and K are in the same group of the periodic table, they could be incorporated into the copper cathode during the electrodeposition process. The presence of sodium could be related to the previous handling processes for performing the electrodeposition. From the atomic absorption analysis, it was determined that the powders were free of sodium and potassium.

Samples annealed at 753 K in the same salts as used in the electrodeposition process, but without electric current circulation, were also studied, in order to differentiate between the thermal and electrical influences on the process.

A summary of the samples studied and their lithium content is tabulated in Table 1. The

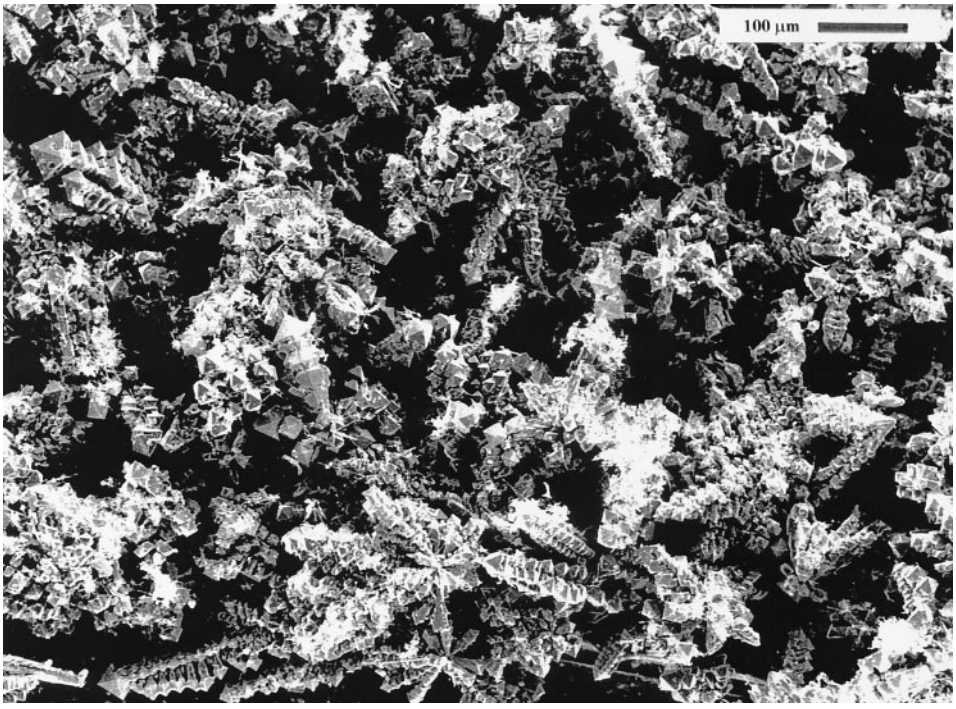

Fig. 1. Scanning electron micrograph of Cu–Li crystals on the copper cathode after electrodeposition.

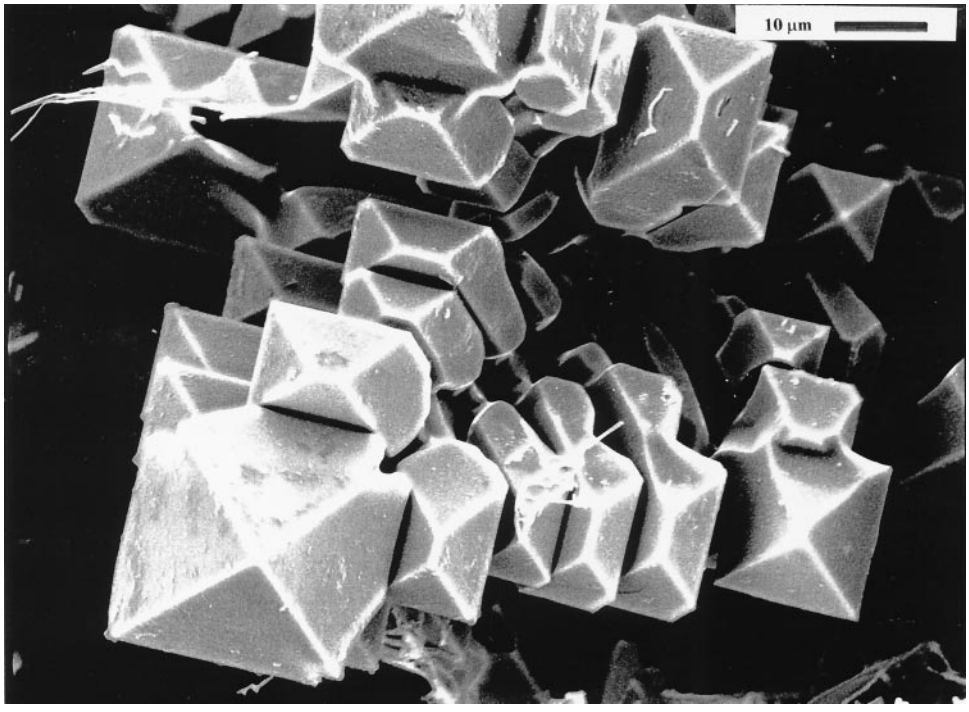

Fig. 2. Details of the geometrical characteristics of the Cu–Li crystals.

Table 1
Lithium content of electrodeposited and annealed samples

Sample description	Electrodeposition time (min)	Annealing time (min)	Lithium content (at%)	Lattice parameter (nm)
(a), pure copper	—	—	—	0.361
(b), only annealed	—	10	—	0.361
(c), only annealed	—	20	—	0.361
(d), electrodeposited	1	—	1.14	0.361
(e), electrodeposited	5	—	1.55	0.361
(f), electrodeposited	15	—	2.57	0.361
(g), electrodeposited	30	—	4.30	0.361
(h), Cu–Li powders	Obtained from samples d–g	—	18.00	0.364

total lithium content of the cathodes (substrate plus Cu–Li powders) for the as-deposited samples, determined by atomic absorption analysis, is also presented in this table. "As-deposited samples" means that the samples were tested with all the layers of crystals on the surface, i.e., the external layers of crystals were not removed by mechanical polishing of the cathodes, as done in earlier work [9,10]. Nevertheless, the samples had nonuniform lithium concentration, and there exists a significant difference between the cathode and the Cu–Li crystals, as shown below.

X-ray diffraction (XRD) measurements were carried out at room temperature, on a Seifert XRD-3000 powder diffractometer, using a constant illuminated area of 10 mm thick. The measurement conditions were 50 kV and 40 mA. All measurements were carried out in the 2θ range of 10°–50°, using Mo radiation. X-ray studies were carried out on both electrodeposited and annealed samples 10×20 mm^2 in area and 0.1 mm thick. The Cu–18at%Li powders were obtained by mechanical polishing the external crystal layers of the electrodeposited cathodes. Electrodeposited cathodes corresponding to different periods of time were used to obtain the powders.

3. Results and discussion

Fig. 3 shows the diffraction patterns of the electrodeposited samples for 1 min (sample d), 5 min (sample e), 15 min (sample f), and 30 min (sample g) of Table 1. To enhance differences, the spectra were plotted in two split ranges. The first range, $10° \leq 2\theta \leq 25°$, is plotted in Fig. 3a, and the second one, $25° \leqslant 2\theta \leqslant 40°$, is plotted in Fig. 3b. In Fig. 3a, for the sample electrodeposited for 1 min (sample d), reflections (111) and (200) related to the copper structure at approximately $2\theta = 19.5°$ and $2\theta = 22.5°$ were found. Small subsidiary peaks to the left of the main copper peaks related to the Cu–18at%Li crystals were also observed. Fig. 3b shows a similar situation of copper peaks and subsidiaries Cu–18at%Li peaks at smaller angles. Reflections (220) and (311) of pure copper at about $2\theta = 32.5°$ and $2\theta = 38°$, respectively, together with the small peaks of Cu–18at%Li located at smaller angles, were observed.

After 1 min of electrodeposition, only reflections (111), (200), (220), and (311) associated

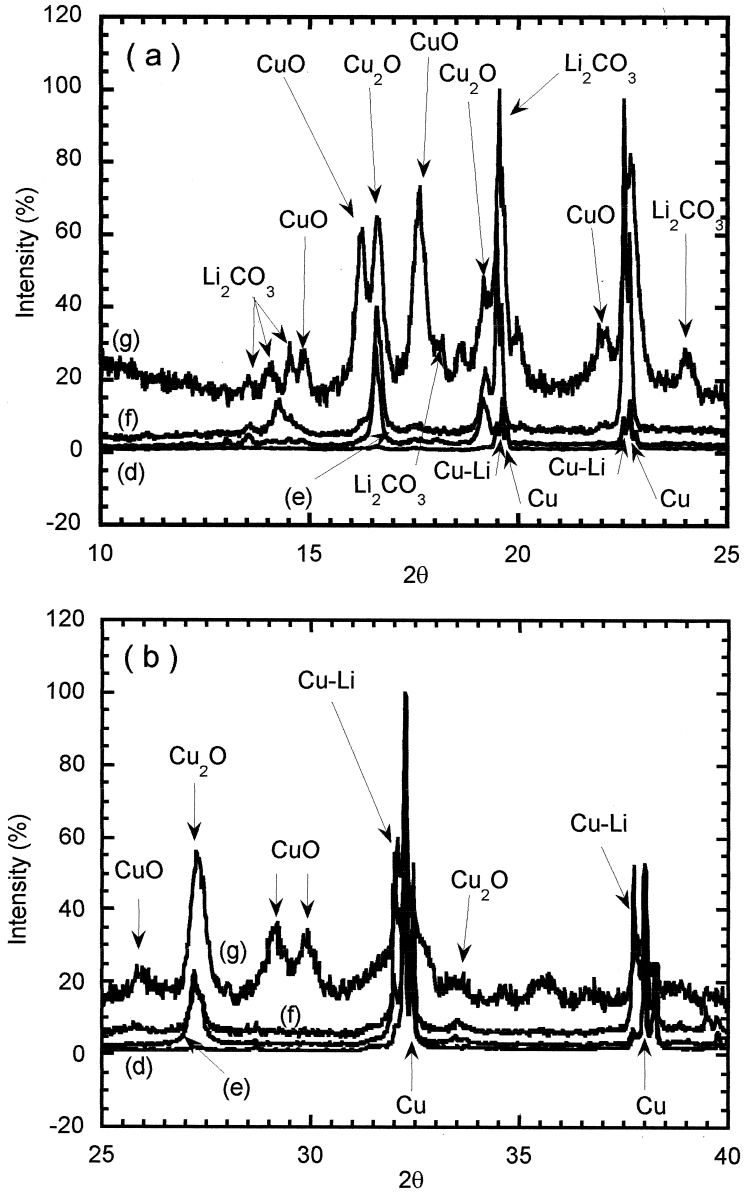

Fig. 3. (a) XRD patterns in reflection between $2\theta = 10°$ and 25°, for samples d to g. The peaks related to the phases of Cu-18%Li, Cu_2O, Li_2CO_3, and CuO are labeled. (b) XRD patterns in reflection between $2\theta = 25°$ and 40°, for samples d to g. The peaks related to Cu–18%Li phases Cu_2O, Li_2CO_3, and CuO are labeled.

with pure Cu and Cu–Li crystals were observed. It is interesting to note that both peaks are split after 1 min of electrodeposition and, therefore, it can be visualized that the change in the lithium concentration was very fast. It could be inferred that the crystals so formed grow with a high lithium concentration. No other phases were detected until 1 min of electrodeposition. For electrodeposition times up to 4 min, reflection peaks related to the Cu_2O oxide

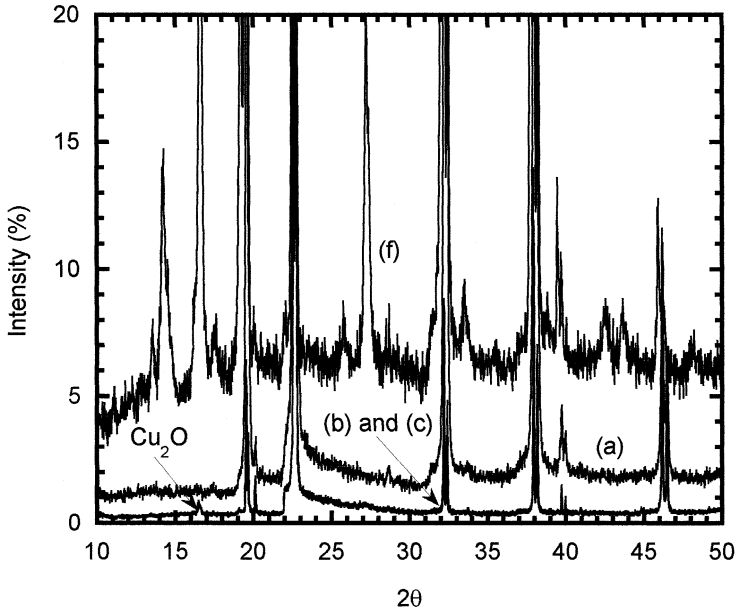

Fig. 4. XRD pattern for samples a, b, c, and f. Patterns related to samples b and c are practically overlapped in the whole 2θ range.

were detected. A small quantity of Li_2CO_3 phase was also observed. Furthermore, the peaks height related to Cu–Li crystals increased. In samples electrodeposited for 15 (sample f) and 30 (sample g) min, the volume fractions of Cu–18at%Li crystals Cu_2O and Li_2CO_3 increased and small quantities of CuO phase also appeared.

The nonvariation in the peak position of the Cu cathode (cell parameter 0.361 nm) with the electrodeposition time can be explained by the following analysis. The crystals with a high lithium content grow fast, while the lithium diffusion far from the inclusions is slow. On the other hand, for Cu–Li crystals, a shift in the peak position (cell parameter 0.364 nm) occurs, showing a diffusion of Li into the Cu matrix.

It may be that both the degree of oxidation and the lithium-carbonate formation increase with the electrodeposition process and thus the increase is a consequence of a thermal process occurring in the fused salts bath during annealing at 753 K and the electrodeposition process. To confirm this, X-ray studies were performed on samples b and c. Fig. 4 shows the diffraction pattern for pure Cu (sample a), Cu annealed in salts for 10 min (sample b) and for 20 min (sample c), and the sample electrodeposited for 15 min (sample f). Samples a and f were plotted to show the striking differences between the two treatments. It can be seen from Fig. 4 that samples b and c only exhibited a small foreign peak at about $2\theta = 16.5°$, which is related to Cu_2O. However, in the case of sample f, Cu_2O, CuO, and Li_2CO_3 peaks are observed. The quantity of copper oxides for a sample annealed 20 min was smaller than that for a sample electrodeposited for 15 min. Therefore, the appearance of copper oxides and lithium carbonates in the cathode is largely related to the electrodeposition process. Thus, the quantity of copper oxides and lithium carbonates could be controlled by electrodeposition time. The evolution of the spectra indicates that the CuO phase is mainly linked to the

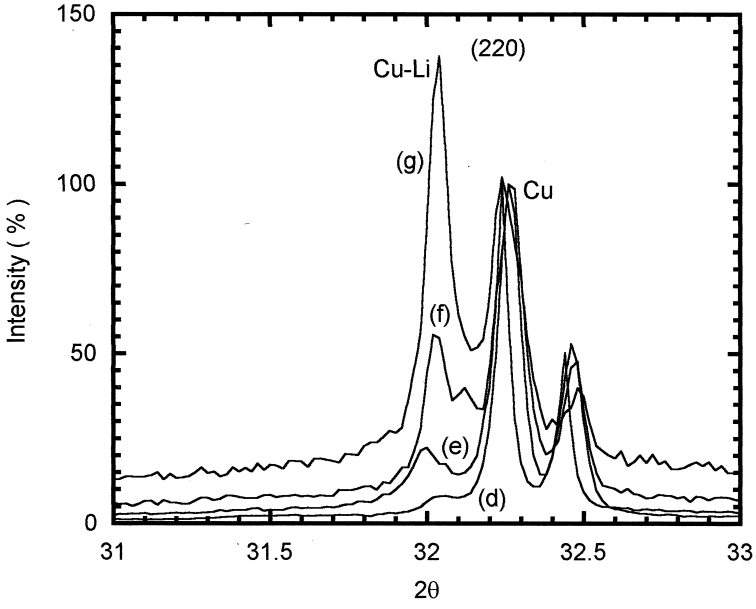

Fig. 5. Evolution of the (220) reflection for the Cu–18at%Li crystals and copper cathode for samples electrodeposited during different periods of time.

electrodeposition process. In contrast, the Cu_2O phase is mainly related to a thermal process, since it appears without electrical current.

The evolution of the volume fraction of Cu–Li crystals for different electrodeposition times was followed by means of XRD studies. Fig. 5 shows the (220) reflections of copper, approximately at $2\theta = 32.25°$, and the (220) reflections of Cu–Li crystals, approximately at $2\theta = 32.05°$, in samples d–g. The X-ray spectra were normalized with respect to the copper (220) peak. The height of the diffraction peak corresponding to the Cu–18at%Li phase increased with electrodeposition time. The integrated intensity of the Cu–Li (220) reflections allows one to determine the evolution of the quantity of deposited crystals. Fig. 6 shows both the quantity of Cu–Li crystals, in arbitrary units, and the total lithium concentration, vs. electrodeposition time.

In order to analyze the diffusion of lithium into the copper cathode, the external layers of Cu–Li crystals were removed by mechanical polishing. Fig. 7 shows the surface of the Cu cathode with inclusions of Cu–Li crystals on the sample surface. These inclusions had a lithium concentration similar to that in the crystals in the external layers, as determined by backscattered electron analysis [9,10].

Fig. 8 shows the (311) reflections corresponding to three different kind of samples: (1) pure copper (sample a); (2) sample g, after removal of both the external layers and inclusions of Cu–Li crystals in the cathode, i.e., the sample g was polished until all the inclusions in the substrate (shown in Fig. 7) were removed; and (3) Cu–Li powder crystals (sample h). The lithium diffusion into the whole cathode, free of the inclusions, would be rather small. In fact, the cell parameter of the pure copper and the electrodeposited cathode after being polished

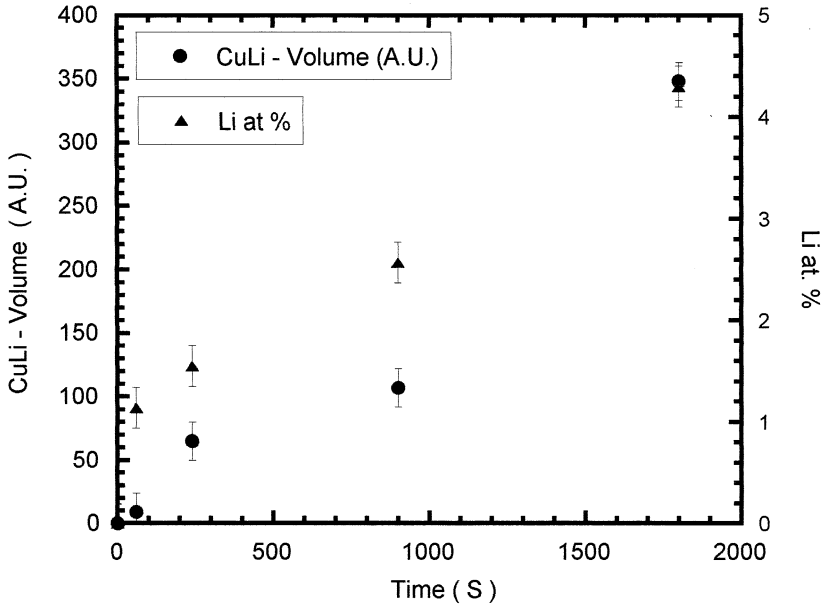

Fig. 6. Cu–18at%Li quantity and total at% Li concentration (from Table 1) vs. electrodeposition time.

are similar, about 0.361 nm. In contrast, the Cu–Li crystals show a larger cell parameter, about 0.364 nm, according to the presence of lithium in solid solution in the copper.

Cu–Li crystals were formed even during 1 min of electrodeposition, as shown in Fig. 3, where the peaks associated with pure Cu and Cu–Li are split. In addition, the Cu–Li crystals had the same lithium content (about 18 at%) [9,10], independent of the electrodeposition time employed in this work. The X-ray diffraction study showed that Cu–Li crystals exhibit a diffraction pattern corresponding to a disordered solid solution of substitutional Li atoms in the Cu matrix (space group *Fm*3*m*). The size of the cell is about 0.364 nm, which is in

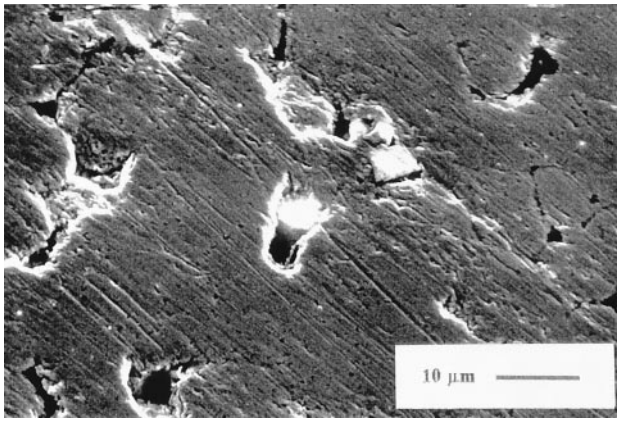

Fig. 7. Scanning electron micrograph of the copper substrate after that the Cu–Li crystals were removed from the surface.

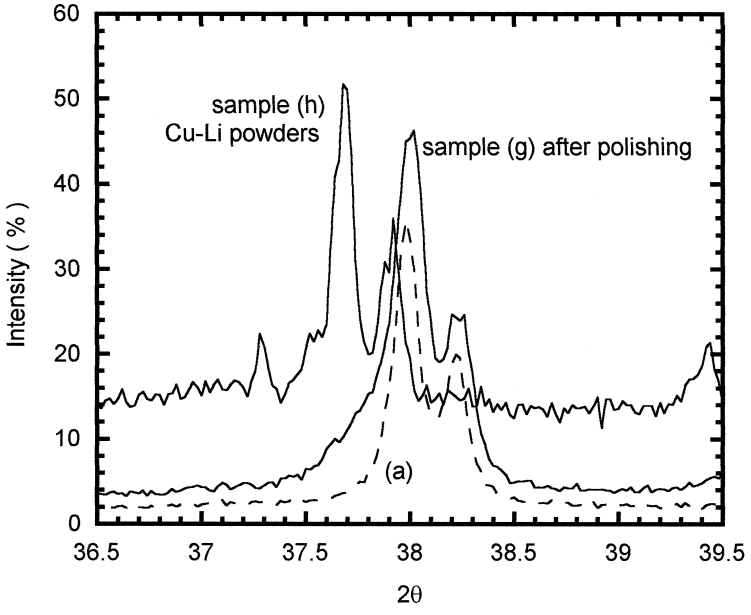

Fig. 8. The (311) reflections corresponding to three different samples: (a) pure Cu, (b) the sample electrodeposited for 30 min (sample g) after removal of the external layers of Cu–Li crystal, and (c) the Cu–Li powder crystals.

agreement with the results reported [12] for this lithium concentration. These results suggest that lithium diffuses quickly into Cu, attaining a maximum lithium concentration. In contrast, the results of Fig. 8 indicate that Li diffusion into Cu bulk, free of the inclusions, is very small.

An approximate calculus of the diffusion coefficient, D, from the activation parameters obtained in the Zener relaxation [13,14] led to a value for D of about 2×10^{-10} cm^2/s at 973 K. It is close to the value of the diffusion coefficient of beryllium in copper [15].The activation energy was estimated to be about 144 KJ/mol and the preexponential factor was about 0.01 cm^2/s. The value of D at the electrodeposition temperature, 753 K, was about 1×10^{-12} cm^2/s. Nevertheless, this calculus does not allow in an easy mode to evaluate the degree of migration of the lithium in the copper matrix. A careful study of lithium diffusion in copper will be reported in a future work.

In order to explain the fast formation of Cu–18at%Li crystals, it is necessary to study the Cu–Li phase diagram showed in Fig. 9 [12]. Lithium addition decreases strongly the solidus–liquidus transformation temperature, changing from 1356 K for pure Cu to about 450 K for Cu-23at%Li. At the electrodeposition temperature (753 K), the maximum lithium content allowed in solid phase is about 18 at%. Thus, diffusion of lithium into the copper cathode promotes a progressive increase of lithium content during the electrodeposition process, but in a narrow layer parallel to the cathode surface. In this layer, the maximum lithium content is quickly achieved and the solid locally transforms to the liquid phase. The liquid phase is metastable and decomposes into solid and liquid phases. The liquid phase is rich in lithium and the solid phase has a limit in the lithium concentration, given by the concentration of it corresponding to the solidus–liquidus curve at this temperature. The result

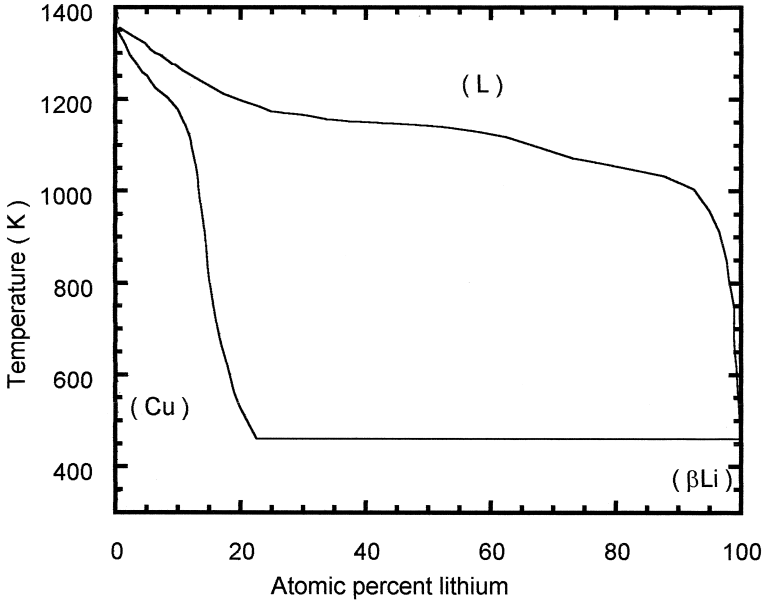

Fig. 9. Cu–Li binary phase diagram.

of this process is the formation of Cu–Li crystals over the copper substrate. Therefore, the increase in the lithium content of the samples with electrodeposition time could be related to an increase in the concentration of Cu–Li crystals, both as inclusions on the cathode surface and as dendrites growing out of the substrate. The proposed mechanism is in agreement with the similar evolution of the lithium content and the quantity of Cu–Li crystals shown in Fig. 6.

Acknowledgments

This work was supported by PEI no. 0116/98 of the National Council of Research Argentina (CONICET), the Centro de Investigación Minera y Metalúrgica, Chile, under contract 005/97 in the framework of a Research of the Universidad Católica de Valparaíso, WCIMM 99UC/213/012, the Escuela de Ingeniería Eléctrica, FCEIA, UNR, Argentina, and the PID-202/1998/99/00 of the UNR, Argentina.

References

[1] K.J. Pascoe, Properties of Materials for Electrical Engineers, John Wiley & Sons, New York, 1973.
[2] J. Ramírez Vázquez, Electrotechnical Materials, CEAC Encyclopedia of Electricity, CEAC Ed., Barcelona, Spain, 1986.
[3] J.T. Edwards, A.J. Hillei, Phil Mag 35 (1977) 1221.
[4] R.J. Rioja, D.E. Laughlin, Acta Metall 28 (1980) 1301.

[5] M. Miki, I. Ogino, Mater Trans JIM 36 (9) (1995) 1118.
[6] A.G. Khachaturyan, D.E. Laughlin, Acta Metall Mater 38 (1990) 1823.
[7] T. Sakai, H. Miura, N. Muramatsu, Mater Trans JIM 36 (8) (1995) 1023.
[8] R.D.K. Misra, C.J. McMahon Jr., A. Guha, Scripta Metall Mater 11 (1994) 1471.
[9] O.A. Lambri, A. Peñaloza, A.V. Morón-Alcain, M. Ortiz, F.C. Lucca, Mater Sci Eng A 212 (1996) 108.
[10] O.A. Lambri, A.V. Morón Alcain, G.I. Lambri, A. Peñaloza, M. Ortiz, C. Wörner, E. Bocanegra, Mater Trans JIM 40 (1) (1999) 72.
[11] A. Peñaloza, M. Ortiz, C.H. Wörner, J Mater Sci Lett 14 (1995) 511.
[12] A.D. Pelton, Bull Phase Diag 7 (2) (1986) 142.
[13] A.S. Nowick, B.S. Berry, Anelastic Relaxation in Crystalline Solids, Academic Press, New York, 1972.
[14] O.A. Lambri, A.V. Moron Alcain, E.D. Bulejes, A. Peñaloza, M. Ortiz, J Phys IV 6 (1996) C8–89.
[15] D.B. Butrymowicz, J.R. Manning, M.E. Read, J Phys Chem Ref Data 4 (1) (1975) 177.